Inorganic Chemistry

Article

pubs.acs.org/IC

Anion-Induced Self-Assembly of Luminescent and Magnetic Homoleptic Cyclic Tetranuclear $Ln_4(Salen)_4$ and $Ln_4(Salen)_2$ Complexes (Ln = Nd, Yb, Er, or Gd)

Weixu Feng,[†] Yao Zhang,[†] Zhao Zhang,[†] Xingqiang Lü,*[,†,‡] Han Liu,[†] Guoxiang Shi,[†] Dan Zou,[†] Jirong Song,[†] Daidi Fan,[†] Wai-Kwok Wong,*[,§] and Richard A. Jones[∥]

[†]Shaanxi Key Laboratory of Degradable Medical Material, Shaanxi Key Laboratory of Physico-inorganic Chemistry, Northwest University, Xi'an 710069, Shaanxi, China

[‡]Fujian Institute of Research on the Structure of Matter, Chinese Academy of Science, Fuzhou 350002, Fujian, China

[§]Department of Chemistry, Hong Kong Baptist University, Waterloo Road, Kowloon Tong, Hong Kong, China

[∥]Department of Chemistry and Biochemistry, The University of Texas at Austin, 1 University Station A5300, Austin, Texas 78712-0165, United States

Supporting Information

ABSTRACT: Unique homoleptic cyclic tetranuclear $Ln_4(Salen)_4$ complexes $[Ln_4(L)_2(HL)_2(\mu_3\text{-}OH)_2Cl_2]\cdot 2Cl$ (Ln = Nd, **1**; Ln = Yb, **2**; Ln = Er, **3**; Ln = Gd, **4**) or $Ln_4(Salen)_2$ complexes $[Ln_4(L)_2(\mu_3\text{-}OH)_2(OAc)_6]$ (Ln = Nd, **5**; Ln = Yb, **6**; Ln = Er, **7**; Ln = Gd, **8**) have been self-assembled from the reaction of the hexadentate Salen-type Schiff-base ligand $\mathbf{H_2L}$ with $LnCl_3\cdot 6H_2O$ or $Ln(OAc)_6\cdot 6H_2O$ (Ln = Nd, Yb, Er, or Gd), respectively ($\mathbf{H_2L}$: *N*,*N*′-bis(salicylidene)cyclohexane-1,2-diamine). The result of their photophysical properties shows that the strong and characteristic NIR luminescence for complexes **1**−**2** and **5**−**6** with emissive lifetimes in microsecond ranges are observed, and the sensitization arises from the excited state (both ^{1}LC and ^{3}LC) of the hexadentate Salen-type Schiff-base ligand with the flexible linker. Temperature dependence (1.8−300 K) magnetic susceptibility studies of the eight complexes suggest the presence of an antiferromagnetic interaction between the Ln^{3+} ions.

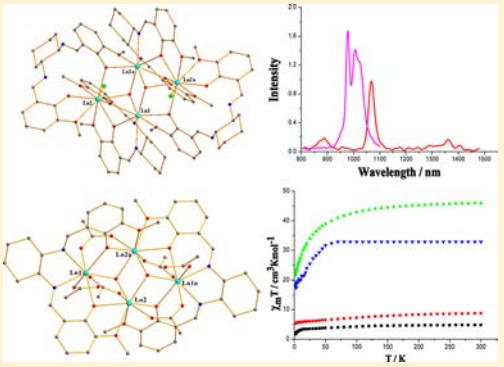

INTRODUCTION

Polynuclear Ln^{3+} complexes with distinct luminescent and magnetic properties are currently of interest because of their potential applications in the preparation of new optical[1] or magnetic materials[2] and ideal probes in biology.[3] However, the control of structures of polynuclear Ln^{3+} complexes is often problematic due to the small energy differences, the high coordination numbers, and the flexible coordination geometries adopted by the Ln^{3+} ions.[4] In fact, the challenge to resolve the problem is strengthened because that construction of the polynuclear Ln^{3+} complexes is distinctively affected by other factors, such as the character of organic ligands,[5] the nature of counterions,[6] and the reaction conditions.[7] Moreover, from the viewpoint of the enhancement of their photophysical properties, it is required that the strong light-harvesting of the organic chromophores, the effective energy transfer from the chromophores to the Ln^{3+} ion, and the minimization of nonradiative processes of the Ln^{3+} ion are achieved,[8] besides complete avoiding or decreasing the luminescent quenching effect arising from OH-, CH-, or NH-oscillators around the Ln^{3+} ion.[9] On the other hand, as to the discrete Ln^{3+}-based clusters as the promising compounds for the development of single-molecule magnets (SMMs),[10] the promotion of magnetic-exchange interactions between Ln^{3+} ions through the overlap of bridging ligands orbitals with their "contracted" 4f orbitals is also a difficult task.[11]

Compared to the amount of efforts on the photophysical[12] or magnetic[13] behavior of 3d−4f heteronuclear complexes from the compartmental Salen-type Schiff-base ligands, the research on luminescent and magnetic polynuclear Ln^{3+} Salen complexes has not been researched nearly as extensively, especially the limited single-crystal X-ray diffraction studies have been reported for those classic complexes.[14] Nonetheless, for the typical quadridentate Salen-type Schiff-base ligands, binuclear triple-decker and trinuclear triple-decker Ln^{3+} complexes[15] are obtained, in which the Salen-type Schiff-base ligand with the rigid linker has been used, their photophysical properties should be further enhanced due to the mismatch of energy levels, despite the chromophores with rigid linkers absorbing at longer wavelength. As to the pure quadridentate Salen-type Schiff-base ligands with flexible linkers, anion-

Received: May 5, 2012
Published: October 8, 2012

   dx.doi.org/10.1021/ic300918c | *Inorg. Chem.* 2012, 51, 11377−11386

dependent discrete binuclear or tetranuclear homoleptic Ln^{3+} complexes[16] and polymeric Ln^{3+} complexes[17] have been reported, while the self-assembly process is complicated and strictly relative to the detailed reaction conditions, besides the diverse quadridentate and bidentate coordination codes adopted. Moreover, the self-assembly from the rigid hexadentate Salen-type Schiff-base ligand with the outer O_2O_2 moiety gives anion-induced trinuclear triple-decker,[18] trinuclear tetra-decker,[19] or pentanuclear tetra-decker[20] Ln^{3+} complexes, in which the luminescent quenching effect that arises from coordinated MeOH or H_2O around the Ln^{3+} ions inevitably exists. To the best of our knowledge, few reports of the self-assembly of polynuclear lanthanide complexes from the flexible hexadentate Salen-type Schiff-base ligand with the outer O_2O_2 moiety have been documented.[21] Moreover, compared with polynuclear Dy^{3+} families, examples of other Ln^{3+}-containing SMMs are still scarce.[22] Herein, starting from the hexadentate Salen-type Schiff-base ligand $\mathbf{H_2L}$ ($\mathbf{H_2L}$ = N,N′-bis(3-methoxy-salicylidene)cyclohexane-1,2-diamine) with the flexible linker, the richness of its coordination codes ($(\mathbf{L})^{2-}$ and $(\mathbf{HL})^{-}$ modes, as shown in Scheme 1) endows the formation of two series of

Scheme 1. Molecular Structure and Bonding Modes of the Salen-Type Schiff-Base Ligand H_2L for Polynuclear Lanthanide Complexes 1−8

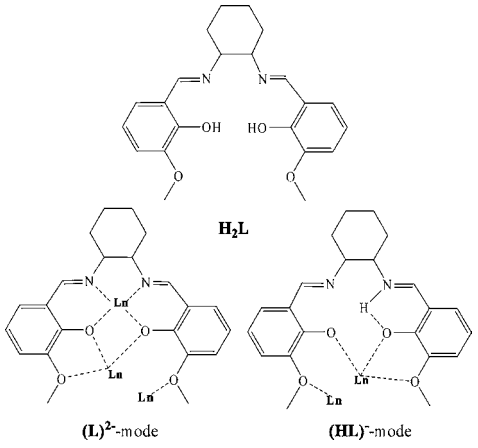

anion-induced homoleptic cyclic tetranuclear $[Ln_4(L)_2(HL)_2(\mu_3\text{-}OH)_2Cl_2]\cdot 2Cl$ (Ln = Nd, **1**; Ln = Yb, **2**; Ln = Er, **3**; Ln = Gd, **4**) and $[Ln_4(L)_2(\mu_3\text{-}OH)_2(OAc)_6]$ (Ln = Nd, **5**; Ln = Yb, **6**; Ln = Er, **7**; Ln = Gd, **8**). The sensitization for the NIR luminescence of the Ln^{3+} ions and the magnetic properties of the homoleptic cyclic tetranuclear $Ln_4(Salen)_4$ or $Ln_4(Salen)_2$ complexes are discussed.

EXPERIMENTAL SECTION

General Methods. All chemicals were commercial products of reagent grade and were used without further purification. Elemental analyses were performed on a Perkin-Elmer 240C elemental analyzer. Infrared spectra were recorded on a Nicolet Nagna-IR 550 spectrophotometer in the region 4000−400 cm^{-1} using KBr pellets. ^1H NMR spectra were recorded on a Bruker Plus 400 spectrometer with $SiMe_4$ as internal standard in CD_3CN at room temperature. ESI-MS was performed on a Finnigan LCQ^{DECA} XP HPLC-MS_n mass spectrometer with a mass to charge (m/z) range of 4000 using a standard electrospray ion source and MeCN as solvent. Electronic absorption spectra in the UV−vis region were recorded with a Cary 300 UV spectrophotometer, and steady-state visible fluorescence, PL excitation spectra on a Photon Technology International (PTI) Alpha scan spectrofluorometer, and visible decay spectra on a pico-N_2 laser system (PTI Time Master). The quantum yield of the visible luminescence for each sample was determined by the relative comparison procedure, using a reference of a known quantum yield (quinine sulfate in dilute H_2SO_4 solution, Φ_{em} = 0.546). NIR emission and excitation in solution were recorded by PTI QM4 spectrofluorometer with a PTI QM4 near-infrared InGaAs detector. The data of magnetic susceptibility were collected using the Quantum Design SQUID MPMS-XL magnetometer from polycrystalline samples at an eternal field of 1000 Oe with the temperature range from 1.8 to 300 K.

X-ray Crystallography. Single crystals of $[Nd_4(L)_2(HL)_2(\mu_3\text{-}OH)_2Cl_2]\cdot 2Cl\cdot 6EtOH$ (**1**·6EtOH), $[Gd_4(L)_2(HL)_2(\mu_3\text{-}OH)_2Cl_2]\cdot 2Cl\cdot 2EtOH\cdot 2H_2O$ (**4**·2EtOH·2H_2O), $[Yb_4(L)_2(\mu_3\text{-}OH)_2(OAc)_6]$ (**6**), and $[Er_4(L)_2(\mu_3\text{-}OH)_2(OAc)_6]$ (**7**) of suitable dimensions were mounted onto thin glass fibers. All the intensity data were collected on a Bruker SMART CCD diffractometer (Mo Kα radiation and λ = 0.710 73 Å) in Φ and ω scan modes. Structures were solved by direct methods followed by difference Fourier syntheses, and then refined by full-matrix least-squares techniques against F^2 using SHELXL-97.[23] All other non-hydrogen atoms were refined with anisotropic thermal parameters. Absorption corrections were applied using SADABS.[24] Hydrogen atoms were placed in calculated positions and refined isotropically using a riding model. CCDC reference numbers 879715 for **1**·6EtOH, and 879617−879619 for **4**·2EtOH·2H_2O and **6**−**7**, respectively.

Synthesis of the Salen-Type Schiff-Base Ligand H_2L (H_2L = *N*,*N*′-Bis(3-methoxy-salicylidene)cyclohexane-1,2-diamine). To a stirred solution of an equimolar mixture of *cis*- and *trans*-1,2-diaminocyclohexane (6.0 mL, 50 mmol) in absolute EtOH (20 mL), *o*-vanillin (15.0 g, 100 mmol) was added, and the resulting mixture was refluxed for 5 h. After cooling to room temperature, the insoluble yellow precipitate was filtered and was recrystallized using absolute EtOH to give a pale yellow polycrystalline solid. Yield: 13.6 g, 71%. Anal. Found: C, 69.01; H, 6.94; N, 7.26. Calcd for $C_{22}H_{26}N_2O_4$: C, 69.09; H, 6.85; N 7.32. IR (KBr, cm^{-1}): 3455 (b), 3058 (w), 2933 (w), 2862 (w), 2597 (w), 1619 (s), 1588 (w), 1470 (s), 1418 (m), 1345 (w), 1251 (vs), 1196 (w), 1168 (w), 1144 (w), 1085 (m), 1036 (w), 984 (m), 953 (w), 894 (w), 849 (m), 776 (w), 731 (m), 668 (w), 616 (w), 595 (w), 568 (w), 516 (w), 467 (w), 422 (w). ^1H NMR (400 MHz, CD_3CN): δ (ppm) 13.84 (s, 2H, OH), 8.24 (s, 2H, CH=N), 6.85 (d, 2H, Ph), 6.78 (d, 2H, Ph), 6.72 (t, 2H, Ph), 3.86 (s, 6H, MeO), 3.32 (m, 2H, Ch), 1.92 (m, 4H, Ch), 1.58 (m, 4H, Ch).

Synthesis of $[Nd_4(L)_2(HL)_2(\mu_3\text{-}OH)_2Cl_2]\cdot 2Cl$ (1). To a stirred solution of $\mathbf{H_2L}$ (0.115 g, 0.3 mmol) in absolute EtOH (8 mL) were added Et_3N (100 μL) and a solution of $NdCl_3\cdot 6H_2O$ (0.3 mmol, 0.107 g) in absolute EtOH (8 mL), respectively. The resultant mixture was refluxed for 2 h, and the clear pale yellow solution was then cooled to room temperature and filtered. Diethyl ether was allowed to diffuse slowly into the filtrate at room temperature, and the pale yellow microcrystal products of **1** were obtained in a few weeks. For **1**: yield 0.080 g, 47%. Anal. Found: C, 46.35; H, 4.49; N, 4.85. Calcd for $C_{88}H_{100}N_8O_{18}Cl_4Nd_4$: C, 46.43; H, 4.43; N, 4.92. IR (KBr, cm^{-1}): 2933 (w), 2862 (w), 1651 (s), 1618 (s), 1553 (w), 1507 (m), 1467 (s), 1451 (s), 1407 (w), 1372 (w), 1344 (w), 1300 (w), 1284 (w), 1236 (m), 1222 (s), 1170 (m), 1143 (w), 1080 (vs), 1069 (s), 984 (m), 946 (w), 902 (w), 857 (w), 784 (w), 743 (m), 657 (w), 576 (w), 534 (w), 496 (w), 473 (w), 442 (w). ^1H NMR (400 MHz, CD_3CN): δ (ppm) 14.61 (s, 2H), 14.18 (s, 2H), 10.21 (t, 4H), 9.51 (t, 4H), 8.63 (d, 4H), 8.32 (d, 4H), 7.63 (m, 4H), 6.51 (m, 4H), 5.42 (m, 6H), 4.63 (m, 6H), 4.01 (m, 4H), 3.85 (m, 4H), 1.73 (s, 6H), 1.33 (s, 6H), 1.18 (m, 4H), 1.06 (m, 4H), −0.13 (m, 4H), −0.47 (m, 4H), −0.87 (m, 4H), −1.27(m, 4H), −1.85 (m, 4H), −2.67 (m, 4H), −2.93 (m, 4H), −5.63 (m, 4H). ESI-MS (in MeCN) m/z: 1102.14 (100%), $[M - (Cl)_2]^{2+}$; 2241.26 (19%), $[M - Cl]^+$.

Synthesis of $[Yb_4(L)_2(HL)_2(\mu_3\text{-}OH)_2Cl_2]\cdot 2Cl$ (2). Complex **2** was prepared in the same way as **1** except that $YbCl_3\cdot 6H_2O$ (0.3 mmol, 0.117 g) was used instead of $NdCl_3\cdot 6H_2O$ (0.3 mmol, 0.107 g). For **2**: yield 0.074 g, 41%. Anal. Found: C, 44.05; H, 4.29; N, 4.54. Calcd for $C_{88}H_{100}N_8O_{18}Cl_4Yb_4$: C, 44.19; H, 4.21; N, 4.68. IR (KBr, cm^{-1}): 2937 (w), 2862 (w), 1652 (s), 1622 (s), 1561 (w), 1506 (m), 1475

dx.doi.org/10.1021/ic300918c | Inorg. Chem. 2012, 51, 11377−11386

Scheme 2. Anion-Induced Formation of Homoleptic Cyclic Tetranuclear $Ln_4(Salen)_4$ and $Ln_4(Salen)_2$ Complexes

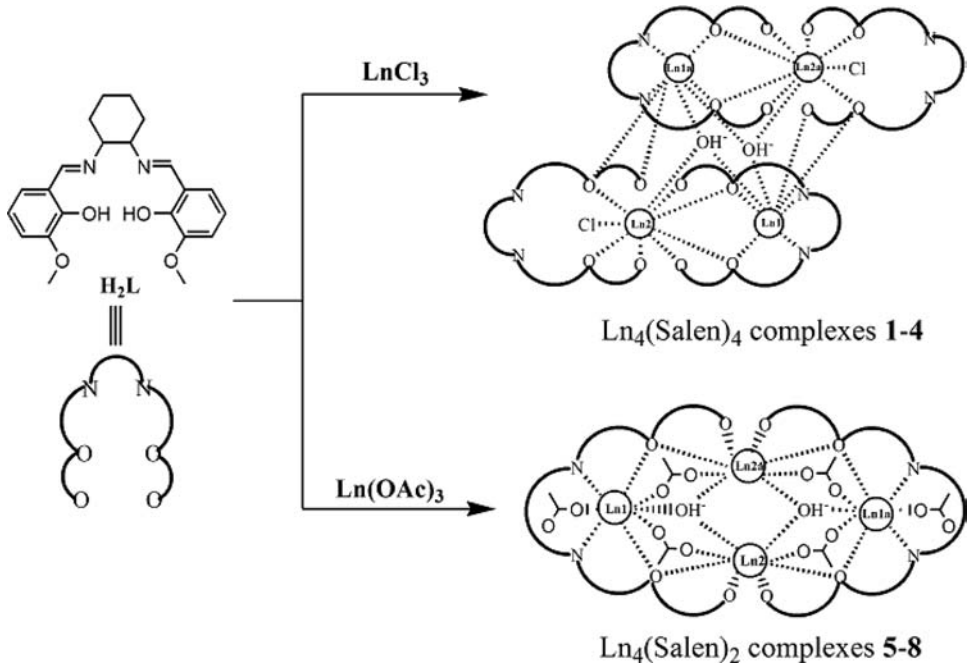

(s), 1456 (s), 1408 (w), 1367 (w), 1345 (w), 1307 (w), 1291 (w), 1230 (m), 1223 (s), 1169 (m), 1144 (w), 1088 (vs), 1071 (s), 983 (m), 952 (w), 904 (w), 858 (w), 783 (w), 742 (m), 662 (w), 578 (w), 539 (w), 483 (w), 461 (w), 435 (w). ESI-MS (in MeCN) *m/z*: 1160.43 (100%), $[M - (Cl)_2]^{2+}$; 2356.64 (23%), $[M - Cl]^+$.

Synthesis of $[Er_4(L)_2(HL)_2(\mu_3\text{-}OH)_2Cl_2]\cdot 2Cl$ (3). Complex **3** was prepared in the same way as **1** except that $ErCl_3\cdot 6H_2O$ (0.3 mmol, 0.115 g) was used instead of $NdCl_3\cdot 6H_2O$ (0.3 mmol, 0.107 g). For **3**: yield 0.071 g, 40%. Anal. Found: C, 44.56; H, 4.32; N, 4.67. Calcd for $C_{88}H_{100}N_8O_{18}Cl_4Er_4$: C, 44.62; H, 4.26; N, 4.73. IR (KBr, cm^{-1}): 2938 (w), 2858 (w), 1650 (s), 1622 (s), 1559 (w), 1505 (m), 1473 (s), 1454 (s), 1408 (w), 1366 (w), 1345 (w), 1307 (w), 1291 (w), 1238 (m), 1226 (s), 1171 (m), 1143 (w), 1078 (vs), 1065 (s), 985 (m), 947 (w), 900 (w), 861 (w), 782 (w), 742 (m), 660 (w), 572 (w), 530 (w), 480 (w), 470 (w), 455 (w). ESI-MS (in MeCN) *m/z*: 1148.87 (100%), $[M - (Cl)_2]^{2+}$; 2333.40 (18%), $[M - Cl]^+$.

Synthesis of $[Gd_4(L)_2(HL)_2(\mu_3\text{-}OH)_2Cl_2]\cdot 2Cl$ (4). Complex **4** was prepared in the same way as **1** except that $GdCl_3\cdot 6H_2O$ (0.3 mmol, 0.112 g) was used instead of $NdCl_3\cdot 6H_2O$ (0.3 mmol, 0.107 g). For **4**: yield 0.086 g, 49%. Anal. Found: C, 45.32; H, 4.38; N, 4.74. Calcd for $C_{88}H_{100}N_8O_{18}Cl_4Gd_4$: C, 45.39; H, 4.33; N, 4.81. IR (KBr, cm^{-1}): 2930 (w), 2860 (w), 1654 (s), 1619 (s), 1550 (w), 1509 (m), 1468 (s), 1454 (s), 1403 (w), 1370 (w), 1348 (w), 1302 (w), 1287 (w), 1232 (m), 1224 (s), 1172 (m), 1148 (w), 1081 (vs), 1071 (s), 983 (m), 941 (w), 900 (w), 859 (w), 781 (w), 742 (m), 659 (w), 573 (w), 531 (w), 491 (w), 472 (w), 452 (w). ESI-MS (in MeCN) *m/z*: 1128.85 (100%), $[M - (Cl)_2]^{2+}$; 2293.32 (15%), $[M - Cl]^+$.

Synthesis of $[Nd_4(L)_2(\mu_3\text{-}OH)_2(OAc)_6]$ (5). To a stirred solution of H_2L (0.115 g, 0.3 mmol) in absolute MeOH (5 mL) were added Et_3N (100 μL) and a solution of $Nd(OAc)_3\cdot 6H_2O$ (0.3 mmol, 0.129 g) in absolute MeOH (5 mL), respectively. The resultant mixture was refluxed for 2 h, then 5 mL of absolute MeCN was added, and the clear pale yellow solution was refluxed another 2 h. After cooling to room temperature, the solution was filtered, and diethyl ether was allowed to diffuse slowly into the filtrate at room temperature. The pale yellow microcrystal products of **5** were obtained in a few weeks. For **5**: yield 0.132 g, 51%. Anal. Found: C, 38.90; H, 4.06; N, 3.18. Calcd for $C_{56}H_{68}N_4O_{22}Nd_4$: C, 38.97; H, 3.97; N, 3.25. IR (KBr, cm^{-1}): 2930 (w), 2862 (w), 2344 (w), 2061 (w), 1662 (m), 1638 (s), 1600 (s), 1563 (s), 1471 (vs), 1422 (s), 1369 (w), 1300 (w), 1244 (w), 1223 (m), 1200 (w), 1178 (w), 1100 (m), 1083 (s), 1020 (w), 987 (m), 863 (m), 789 (w), 761 (w), 747 (m), 656 (m), 609 (w), 595 (w), 548 (m), 471 (w), 463 (w). ^1H NMR (400 MHz, CD_3CN): δ (ppm) 15.03 (s, 2H), 14.38 (s, 2H), 12.10 (t, 4H), 11.29 (t, 4H), 9.80 (d, 2H), 9.07 (d, 2H), 8.43 (m, 2H), 8.22 (m, 2H), 7.33 (m, 6H), 7.00 (m, 6H), 6.37 (m, 2H), 6.03 (m, 2H), 4.68 (s, 6H), 3.85 (s, 6H), 3.67 (m, 3H), 3.44 (m, 3H), 3.09 (m, 2H), 2.65 (m, 2H), 1.37 (m, 2H), 0.61 (m, 2H), −0.92 (m, 1H), −1.58 (m, 1H), −2.90 (m, 2H), −3.10 (m, 2H). ESI-MS (in MeCN) *m/z*: 1727.14 (100%), $[M + H]^+$; 804.02 (15%), $[M - (OAc)_2]^{2+}$.

Synthesis of $[Yb_4(L)_2(\mu_3\text{-}OH)_2(OAc)_6]$ (6). Complex **6** was prepared in the same way as **5** except that $Yb(OAc)_3\cdot 6H_2O$ (0.3 mmol, 0.138 g) was used instead of $Nd(OAc)_3\cdot 6H_2O$ (0.3 mmol, 0.129 g). For **6**: yield 0.146 g, 53%. Anal. Found: C, 36.47; H, 3.77; N, 3.02. Calcd for $C_{56}H_{68}N_4O_{22}Yb_4$: C, 36.53; H, 3.72; N, 3.04. IR (KBr, cm^{-1}): 2934 (w), 2862 (w), 2352 (w), 2068 (w), 1660 (m), 1640 (s), 1601 (s), 1561 (s), 1468 (vs), 1420 (s), 1361 (w), 1307 (w), 1239 (w), 1220 (m), 1207 (w), 1171 (w), 1105 (m), 1080 (s), 1027 (w), 981 (m), 859 (m), 782 (w), 758 (w), 744 (m), 652 (m), 616 (w), 590 (w), 542 (m), 475 (w), 453 (w). ESI-MS (in MeCN) *m/z*: 1842.34 (100%), $[M + H]^+$; 861.62 (11%), $[M - (OAc)_2]^{2+}$.

Synthesis of $[Er_4(L)_2(\mu_3\text{-}OH)_2(OAc)_6]$ (7). Complex **7** was prepared in the same way as **5** except that $Er(OAc)_3\cdot 6H_2O$ (0.3 mmol, 0.136 g) was used instead of $Nd(OAc)_3\cdot 6H_2O$ (0.3 mmol, 0.129 g). For **7**: yield 0.147 g, 54%. Anal. Found: C, 36.93; H, 3.83; N, 3.04. Calcd for $C_{56}H_{68}N_4O_{22}Er_4$: C, 36.99; H, 3.77; N, 3.08. IR (KBr, cm^{-1}): 2976 (w), 2936 (w), 2390 (w), 2053 (w), 1662 (m), 1635 (s), 1600 (s), 1556 (s), 1460 (vs), 1416 (s), 1348 (w), 1310 (w), 1244 (w), 1224 (m), 1206 (w), 1170 (w), 1101 (m), 1088 (s), 1027 (w), 995 (m), 864 (m), 785 (w), 757 (w), 742 (m), 644 (m), 616 (w), 588 (w), 540 (m), 469 (w), 457 (w). ESI-MS (in MeCN) *m/z*: 1819.22 (100%), $[M + H]^+$; 850.06 (9%), $[M - (OAc)_2]^{2+}$.

Synthesis of $[Gd_4(L)_2(\mu_3\text{-}OH)_2(OAc)_6]$ (8). Complex **8** was prepared in the same way as **5** except that $Gd(OAc)_3\cdot 6H_2O$ (0.3 mmol, 0.133 g) was used instead of $Nd(OAc)_3\cdot 6H_2O$ (0.3 mmol, 0.129 g). For **8**: yield 0.128 g, 48%. Anal. Found: C, 37.76; H, 3.90; N, 3.12. Calcd for $C_{56}H_{68}N_4O_{22}Gd_4$: C, 37.83; H, 3.85; N, 3.15. IR (KBr, cm^{-1}): 2935 (w), 2860 (w), 2355 (w), 2061 (w), 1669 (m), 1642 (s), 1600 (s), 1559 (s), 1463 (vs), 1417 (s), 1352 (w), 1302 (w), 1231 (w), 1221 (m), 1201 (w), 1170 (w), 1105 (m), 1088 (s), 1025 (w), 963 (m), 861 (m), 780 (w), 757 (w), 742 (m), 657 (m), 619 (w), 588 (w), 542 (m), 477 (w), 465 (w), 437 (w). ESI-MS (in MeCN) *m/z*: 1779.18 (100%), $[M + H]^+$; 830.04 (12%), $[M - (OAc)_2]^{2+}$.

dx.doi.org/10.1021/ic300918c | *Inorg. Chem.* 2012, 51, 11377−11386

Table 1. Crystal Data and Structure Refinement for Complexes 1·6EtOH, 4·2EtOH·2H$_2$O, and 6−7

compd	1·6EtOH	4·2EtOH·2H$_2$O	6	7
formula	$C_{100}H_{136}N_8O_{24}Cl_4Nd_4$	$C_{92}H_{116}N_8O_{22}Cl_4Gd_4$	$C_{56}H_{68}N_4O_{22}Yb_4$	$C_{56}H_{68}N_4O_{22}Er_4$
fw	2552.93	2456.73	1841.30	1818.18
cryst syst	monoclinic	monoclinic	triclinic	triclinic
space group	$P2_1/n$	$P2_1/n$	$P\bar{1}$	$P\bar{1}$
a, Å	18.5179(14)	18.506(3)	11.833(2)	11.824(3)
b,Å	16.1970(12)	16.011(2)	12.133(2)	12.126(3)
c, Å	19.1175(14)	18.964(3)	12.696(3)	12.717(3)
α, deg	90	90	104.541(4)	104.693(5)
β, deg	95.4820(10)	95.885(2)	91.386(4)	91.462(5)
γ, deg	90	90	95.173(3)	95.205(5)
V, Å^3	5707.8(7)	5589.5(15)	1755.2(6)	1754.3(8)
Z	2	2	1	1
D_{calcd}, g cm^{-3}	1.485	1.460	1.742	1.721
cryst size, mm^3	0.30 × 0.25 × 0.22	0.29 × 0.24 × 0.19	0.27 × 0.24 × 0.20	0.28 × 0.23 × 0.21
temp, K	273(2)	273(2)	296(2)	296(2)
F(000)	2584	2448	888	880
μ, mm^{-1}	1.951	2.502	5.349	4.804
θ range, deg	1.46−32.22	1.62−31.28	1.66−26.09	1.66−26.24
reflns measd	56 090	57 530	9401	9404
reflns used	18 813	17 824	6734	6784
params	632	586	389	388
R ($I > 2\sigma(I)$)	R1 = 0.0518	R1 = 0.0675	R1 = 0.0766	R1 = 0.0832
	wR2 = 0.1413	wR2 = 0.2007	wR2 = 0.2116	wR2 = 0.2157
R (all data)	R1 = 0.0723	R1 = 0.0964	R1 = 0.1224	R1 = 0.1414
	wR2 = 0.1634	wR2 = 0.2292	wR2 = 0.2523	wR2 = 0.2638
S	1.110	1.078	1.031	1.023

RESULTS AND DISCUSSION

As shown in Scheme 2, reaction of equimolar amounts of the deprotonated $\mathbf{L}^{2-}$ ligand and $LnCl_3·6H_2O$ (Ln = Nd, Yb, Er or Gd) in refluxing absolute EtOH produced the yellow solution, from which the series of tetranuclear $Ln_4(Salen)_4$ complexes $[Ln_4(L)_2(HL)_2(\mu_3\text{-}OH)_2Cl_2]·2Cl$ (Ln = Nd, **1**; Ln = Yb, **2**; Ln = Er, **3** or Ln = Gd, **4**) were isolated as yellow microcrystalline solids, respectively. Reaction of equimolar amounts of the deprotonated $\mathbf{L}^{2-}$ ligand and $Ln(OAc)_3·6H_2O$ (Ln = Nd, Yb, Er or Gd) in refluxing absolute MeOH−MeCN resulted in the formation of the series of tetranuclear $Ln_4(Salen)_2$ complexes $[Ln_4(L)_2(\mu_3\text{-}OH)_2(OAc)_6]$ (Ln = Nd, **5**; Ln = Yb, **6**; Ln = Er, **7** or Ln = Gd, **8**), respectively. Similar to the good solubility of the Salen-type Schiff-base ligand $\mathbf{H_2L}$ in common organic solvents except for water, complexes **5**−**8** are also soluble in absolute MeCN due to the use of the Salen-type Schiff-base ligand $\mathbf{H_2L}$ with the flexible linker, while the better solubility for the series of complexes **1**−**4** should be further assigned to the charge of the two components (the cationic $[Ln_4(L)_2(HL)_2(\mu_3\text{-}OH)_2Cl_2]^{2+}$ part and two Cl^- anions) in each of the four complexes.

The ligand $\mathbf{H_2L}$ and the two series of eight complexes **1**−**8** were well characterized by EA, FT-IR, ^{1}H NMR, and ESI-MS. In the FT-IR spectra, the characteristic strong absorptions of the ν(C═N) vibration at 1650−1654 cm^{-1} for complexes **1**−**4**, or 1635−1642 cm^{-1} for complexes **5**−**8**, are slightly blue-shifted by the range 31−35 or 16−23 cm^{-1} relative to that of the free Salen-type Schiff-base ligand $\mathbf{H_2L}$ (1619 cm^{-1}) upon the coordination of the Ln^{3+} ions. For complexes **5**−**8**, two additional strong characteristic absorptions at 1600−1601 and 1417−1422 cm^{-1} were observed, which are tentatively attributed to the ν_{as} vibration and the ν_s vibration of OAc^- anions, respectively.[25] As to the room temperature ^{1}H NMR spectra in CD_3CN of complexes **1** and **5**, large shifts (δ from 14.61 to −5.63 ppm for **1** and 15.03 to −3.10 ppm for **5**) of two sets of the proton resonances of the $\mathbf{L}^{2-}$ ligands endowed from the observed $(\mathbf{L})^{2-}$ and/or $(\mathbf{HL})^-$ modes in the molecular structures are observed, due to the Nd^{3+}-induced shift,[26] significantly spread in relative to those of the free $\mathbf{H_2L}$ ligand (δ from 13.84 to 1.58 ppm). The ESI-MS spectra of the two series of complexes (**1**−**4** and **5**−**8**) in MeCN display the respective similar patterns and exhibit the strong mass peak at m/z 1102.14 (**1**), 1160.43 (**2**), 1148.87 (**3**), or 1128.85 (**4**), and 1727.14 (**5**), 1842.34 (**6**), 1819.22 (**7**), or 1779.18 (**8**), assigned to the major species $[Ln_4(L)_2(HL)_2(\mu_3\text{-}OH)_2Cl_2]^{2+}$ of complexes **1**−**4** and $[Ln_4(L)_2(\mu_3\text{-}OH)_2(OAc)_6\text{-}H]^+$ of complexes **5**−**8**, respectively. These observations further indicate that the respective discrete homoleptic $Ln_4(Salen)_4$ or $Ln_4(Salen)_2$ unit is retained in the respective dilute MeCN solution.

The solid state structure of **1**·6EtOH or **4**·2EtOH·2H$_2$O as the representative of **1**−**4** and **6** or **7** as the representative of **5**−**8** was determined by X-ray single-crystal diffraction analysis. Crystallographic data for the four complexes are presented in Table 1, and selected bond lengths and angles are given in Table 1S in the Supporting Information.

Complex **1**·6EtOH crystallizes in the monoclinic space group $P2_1/n$. For complex **1**·6EtOH, the structural unit is composed of one cation $[Nd_4(L)_2(HL)_2(\mu_3\text{-}OH)_2Cl_2]^{2+}$, two free Cl^- anions, and six solvates EtOH. As shown in Figure 1, for the cationic $[Nd_4(L)_2(HL)_2(\mu_3\text{-}OH)_2Cl_2]^{2+}$ part lying about an inversion center, two equivalent $Nd_2(L)(HL)$ moieties are bridged by two μ-O phenoxide atoms (O7 and O7a) of two Salen-type Schiff-base $(\mathbf{HL})^-$ ligands with O_4 tetradentate mode ($(\mathbf{HL})^-$ mode, as shown in Scheme 1) and two O atoms (O9 and O9a) of two coordinated μ_3-OH^- groups, resulting in the

dx.doi.org/10.1021/ic300918c | Inorg. Chem. 2012, 51, 11377−11386

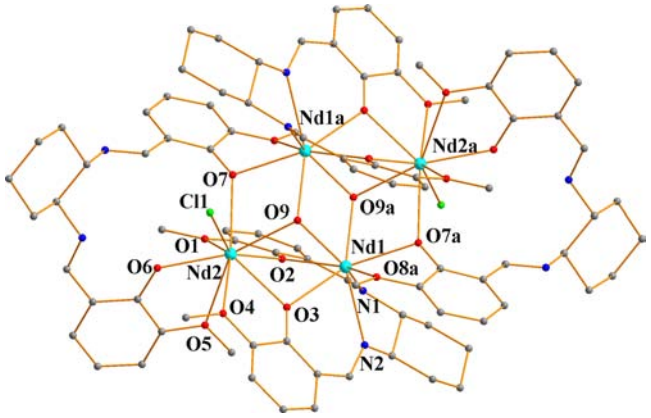

Figure 1. Perspective drawing of the cationic part in complex **1**·6EtOH. Free anions, H atoms, and solvates are omitted for clarity.

formation of a homoleptic cyclic tetranuclear ($Nd_4(Salen)_4$) host structure. In each of two equivalent $Nd_2(L)(HL)$ moieties, two Nd^{3+} (Nd1 and Nd2) ions with different coordination environments also linked by two μ-O phenoxide atoms (O2 and O3) of one Salen-type Schiff-base $(\mathbf{L})^{2-}$ ligand with N_2O_4 hexadentate mode ($(\mathbf{L})^{2-}$ mode) and one O atom (O9) of the coordinated μ_3-OH^- group. The unique inner Nd^{3+} ion (Nd1) is eight-coordinate and bound by the N_2O_2 core of the Salen-type Schiff-base $(\mathbf{L})^{2-}$ ligand in addition to two O atoms (O8a of MeO group and O7a of μ-O phenoxide atom) from the Salen-type Schiff-base $(\mathbf{HL})^{-}$ ligand and two O atoms (O9 and O9a) of two coordinated μ_3-OH^- groups. However, the outer Nd^{3+} ion (Nd2) is nine-coordinate: in addition to the seven oxygen atoms from the two outer O_2O_2 moieties of the two Salen-type Schiff-base ligands, where four O atoms (two of MeO groups and two of phenoxide atoms) are from the Salen-type Schiff-base $(\mathbf{L})^{2-}$ ligand and three O atoms (one of MeO groups and two of phenoxide atoms) from the Salen-type Schiff-base $(\mathbf{HL})^{-}$ ligand, it saturates its coordination environment with one O atom (O9) from the coordinated μ_3-OH^- group and one Cl^- anion (Cl1). Three unique Nd···Nd distances are different at 3.6624(4), 3.8384(5), and 3.9892(4) Å for Nd1···Nd2, Nd1···Nd1a, and Nd1···Nd2a, respectively, in which each of the Nd1···Nd2 separations in the equivalent $Nd_2L(HL)$ moieties is slightly shorter than that (Nd1···Nd1a or Nd1···Nd2a separation) between two equivalent $Nd_2L(HL)$ moieties. It is interesting to notice, as to the charge balance to the cationic $[Nd_4(L)_2(HL)_2(\mu_3\text{-}OH)_2Cl_2]^{2+}$ part, it should be balanced by the protonation of one (N4 or N4a) of the imino nitrogen atoms for two of the four deprotonated Salen-type Schiff-base $(\mathbf{L})^{2-}$ ligands, which endows the formation of two strong intramolecular N3−H3···O6 (2.603(5) Å and 135.6(3)°) H-bond interactions shown in Figure 1S. The two free Cl^- anions and the six solvate EtOH molecules of complex **1**·6EtOH are not bound to the framework, and they exhibit no observed interactions with the host structure. X-ray structural analysis indicated that complex **4**·2EtOH·$2H_2O$ is isomorphous with complex **1**·6EtOH, as shown in Figure 2S, and the similar strong intramolecular H-bond interactions with the short N3−H3···O6 distances (2.610(10) Å) and the reasonable N3−H3···O6 bond angle (134.7(5)°) in the cationic $[Gd_4(L)_2(HL)_2(\mu_3\text{-}OH)_2Cl_2]^{2+}$ host structure are observed in Figure 3S. The two free Cl^- anions and solvates EtOH and H_2O molecules of complex **4**·2EtOH·$2H_2O$ are not bound to the framework, and they also exhibit no observed interactions with the host structure. The slight variation of the detailed structures in the complexes **1**·6EtOH and **4**·2EtOH·$2H_2O$ isolated under the same reaction conditions should be due to the effect of lanthanide contraction.[27]

Complex **6** crystallizes in the triclinic space group $P\bar{1}$. A view of the crystal structure of complex **6** is shown in Figure 2, and

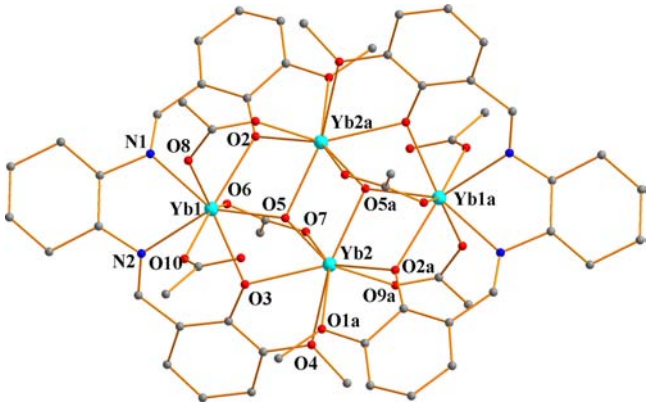

Figure 2. Perspective drawing of complex **6**. H atoms are omitted for clarity.

reveals a tetranuclear centrosymmetric core with two equivalent Yb_2L moieties linked by two μ_3-OH^- groups, two bridged OAc^- anions, and two μ-O phenoxide atoms (O2 and O2a) of the Salen-type Schiff-base $(\mathbf{L})^{2-}$ ligand. In each of two equivalent Yb_2L moieties, two Yb^{3+} (Yb1 and Yb2) ions with different coordination environments also linked by the μ-O phenoxide atom (O3) of the Salen-type Schiff-base $(\mathbf{L})^{2-}$ ligand with N_2O_4 hexadentate mode ($(\mathbf{L})^{2-}$ mode), another bridged OAc^- anion, and one O atom (O5) of the coordinated μ_3-OH^- group. The unique inner Yb^{3+} ion (Yb1) is eight-coordinate and bound by the N_2O_2 core of the Salen-type Schiff-base $(\mathbf{L})^{2-}$ ligand in addition to one O atoms (O5) of the coordinated μ_3-OH^- groups and three O atoms (O6, O8, and O10) from two bridged OAc^- anions and one monodentate OAc^- anion, respectively. For the outer Yb^{3+} ion (Yb2), although it also has the eight-coordinate, its coordination environment is saturated by eight O atoms, with four O atoms (O1a, O2a, O3, and O4) from the two outer O_2O_2 moieties of the two Salen-type Schiff-base ligands, two O atoms (O5 and O5a) from two coordinated μ_3-OH^- groups, and two O atoms (O7 and O9a) from two bridged OAc^- anions. Three unique Yb···Yb distances are different at 3.5761(11), 3.6826(12), and 3.7103(12) Å for Yb1···Yb2, Yb1···Yb2a, and Yb2···Yb2a, respectively, in which each of the Yb1···Yb2 separations in the equivalent Yb_2L moieties is slightly shorter than that (Yb1···Yb2a or Yb2···Yb2a separation) between two equivalent Yb_2L moieties. When Yb^{3+} ion was replaced by Er^{3+} ion, the isomorphous complex **7** was obtained. As shown in Figure 4S and Table 1S, the slight variation of the detailed structures in complexes **6**−**7**, isolated under the same reaction conditions, should also be due to the effect of lanthanide contraction.[27]

In a comparison of complexes **1**·6EtOH and **4**·2EtOH·$2H_2O$ with complexes **6**−**7**, the use of different anions (Cl^- or OAc^-) is critical to the formation of the homoleptic cyclic tetetranuclear $Ln_4(Salen)_4$ or $Ln_4(Salen)_2$ complexes. The common feature in both structures is the retention of one Cl^- or monodentate OAc^- per inner Ln^{3+} ion which is bound to the central N_2O_2 core of one Salen-type Schiff-base ligand.

dx.doi.org/10.1021/ic300918c | *Inorg. Chem.* 2012, 51, 11377−11386

Two equivalent $Ln_2(L)(HL)$ or Ln_2L moieties are also bridged by two coordinated μ_3-OH^- groups to endow the homoleptic cyclic tetranuclear host frameworks, and no solvent molecules found in the host structures are bound to the Ln^{3+} center. In the formation of $Ln_4(Salen)_2$ complexes **6**–**7**, due to the hard Lewis acidity of Ln^{3+} ions, the excess OAc^- anions are able to coordinate effectively to the Ln^{3+} ions and prevent the further coordination of the ligands. Moreover, the structure formation for complexes **1**·6EtOH and **4**·2EtOH·2H_2O also resulted from the flexibility of the ligand, where both $(HL)^-$ and $(L)^{2-}$ coordination modes are incorporated for the stability of the $Ln_4(Salen)_4$ complexes. It is worth noting that the homoleptic cyclic tetranuclear $Ln_4(Salen)_4$ or $Ln_4(Salen)_2$ host structure is distinctively different from the reported structures of binuclear triple-decker,[15] trinuclear triple-decker,[15,18] trinuclear tetra-decker,[19] or pentanuclear tetra-decker Ln^{3+} complexes[20] based on the Salen-type Schiff-base ligands with the rigid linkers, which should be due to the use of the flexible Salen-type Schiff-base ligand **H_2L** with the outer O_2O_2 moiety. On the other hand, the formation of homoleptic cyclic tetranuclear ($Ln_4(Salen)_4$) framework of complexes **1**–**4** appears to be Cl^- anion-dependent, which is comparable to NO_3^- anion-dependent $Ln_4(Salen)_4$ complexes from the same ligand in our recent report,[21] while the OAc^- inducement should dominate the $Ln_4(Salen)_2$ strucutres in complexes **5**–**8**. It is of special interest to compare the self-assembly of the two series of $Ln_4(Salen)_4$ and $Ln_4(Salen)_2$ complexes with that of the reported $Tb_4(Salen)_6$ complex.[16] Although the similar tetranuclear framework is obtained necessarily from the Salen-type Schiff-base ligands with flexible linkers, the character of the Salen-type Schiff-base ligand **H_2L** with both the inner N_2O_2 core and the outer O_2O_2 moiety in complexes **1**–**8**, instead of the pure Salen-type Schiff-base ligand without the outer O_2O_2 moiety in the reported $Tb_4(Salen)_6$ complex,[16] endows the unusual formation of anion-dependent homoleptic cyclic tetranuclear frameworks.

Photophysical Properties of Lanthanide Complexes. The photophysical properties of the ligand **H_2L** and complexes **1**–**4** have been examined in dilute MeCN solution at room temperature or 77 K, and summarized in Table 2 and Figures 3–5. As shown in Figure 3, the similar ligand-centered solution absorption spectra (226–230, 268–269, and 338–342 nm) of complexes **1**–**4** in the UV–vis region are observed, red-shifted upon the coordination of the Ln^{3+} ions as compared to that (220, 260, and 332 nm) of the ligand **H_2L** in MeCN. The molar absorption coefficients of complexes **1**–**4** in all the lowest energy bands (338–342 nm) are almost 4 orders of magnitude larger than that (332 nm) of the ligand **H_2L** due to the involvement of four chromophores. For complexes **1**–**3**, the similar weak visible emissions (ca. λ_{em} = 526 nm and τ < 1 ns) with low quantum yields ($\Phi_{em} < 10^{-5}$) are observed in dilute MeCN solution at room temperature. In addition to the residual weak visible emission, as shown in Figure 4, photo excitation of the chromophore in the range 200–480 nm (λ_{ex} = 401 nm for **1** or 354 nm for **2**) gives rise to the characteristic ligand-field splitting emissions of the Nd^{3+} ion ($^4F_{3/2} \rightarrow {}^4I_{J/2}$, J = 9, 11, 13) or the Yb^{3+} ion ($^2F_{5/2} \rightarrow {}^2F_{7/2}$) in the NIR range, respectively. For complex **1**, the emissions at 888, 1068, and 1361 nm can be assigned to $^4F_{3/2} \rightarrow {}^4I_{9/2}$, $^4F_{3/2} \rightarrow {}^4I_{11/2}$, and $^4F_{3/2} \rightarrow {}^4I_{13/2}$ transitions of the Nd^{3+} ion, respectively, and the emission at 979 nm can be attributed to $^2F_{5/2} \rightarrow {}^2F_{7/2}$ transition of the Yb^{3+} ion for complex **2**. Moreover, unlike that for complex **1** or **2**, the characteristic NIR emission of the Er^{3+} ion for complex **3** cannot be observed. The free ligand **H_2L** or complex **4** also does not exhibit the NIR emission under the same condition, and just displays the typical strong luminescence of the Salen-type Schiff-base ligand in the visible range, as shown in Figure 5. The excitation spectra of complexes **1**–**2**, monitored at the respective NIR emission peak (1068 nm for **1** or 979 nm for **2**), are similar to those monitored at their respective visible emission peak, which clearly demonstrates that both the NIR and visible emissions for complexes **1**–**2** originated from the same π–π^* transitions of the ligand **H_2L**, and the energy transfer from the chromophore to the Ln^{3+} ions takes place efficiently.[28] As a reference compound, complex **4** endows the further study of the chromophore luminescence in the absence of energy transfer, because the Gd^{3+} ion has no energy levels below 32 000 cm^{-1}, and thus cannot accept any energy from the excited

Table 2. Photophysical Properties of the H_2L and Complexes 1–8 at 1 × 10^{-5} M in Absolute MeCN Solution at Room Temperature or 77 K

compd	absorption λ_{ab}/nm [log(ε/dm^3 mol^{-1} cm^{-1})]	excitation λ_{ex}/nm	emission λ_{em}/nm (τ, Φ × 10^3)
H_2L	220(0.84), 260(0.40), 332(0.10)	303, 321, 370	362(1.22 ns, 0.23), 478(1.57 ns, 0.25)
1	228(2.89), 268(1.31), 342(0.45)	374(sh), 401	525(w); 888(1.53 μs), 1068(1.57 μs), 1361 (1.55 μs)
2	230(2.63), 268(1.14), 342(0.44)	354, 395(sh)	527(w); 979(14.77 μs)
3	228(2.53), 269(1.15), 338(0.43)	403	524(w); *a*
4	226(2.88), 268(1.32), 340(0.45)	406	526(0.77 ns, 0.67)
			507(3.2 ns, 77 K), 565(7.5 ms, 77 K)
5	234(1.05), 276(0.48), 346(0.21)	383	490(w); 900(1.44 μs), 1063(1.47 μs), 1332 (1.46 μs)
6	228(1.31), 270(0.57), 346(0.21)	387	483(w); 978(13.82 μs)
7	233(1.05), 275(0.48), 345(0.21)	385	486(w); *a*
8	227(1.20), 269(0.52), 343(0.19)	384	487(0.64 ns, 0.58)
			473(2.5 ns, 77 K), 552(6.4 ms, 77 K)

[a]The emission is too weak to be detected.

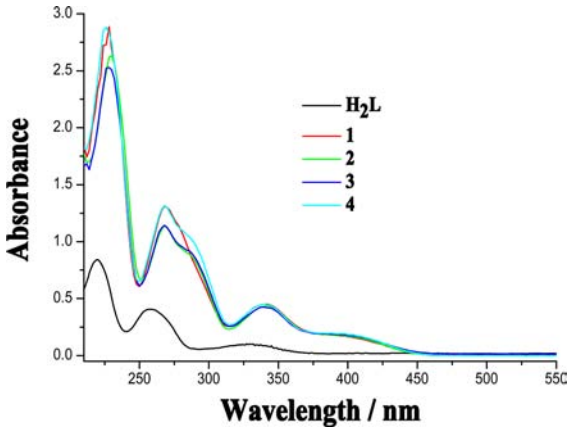

Figure 3. UV–vis absorption spectra of the ligand **H_2L** and complexes **1**–**4** in MeCN solution at 1 × 10^{-5} M at room temperature.

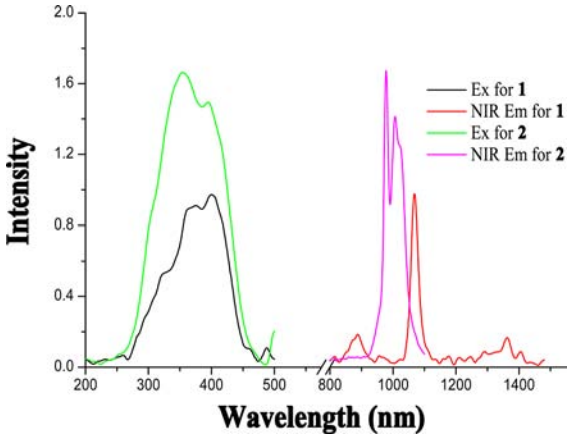

Figure 4. NIR emission and excitation spectra of complexes **1**−**2** in MeCN solution at 1×10^{-5} M at room temperature.

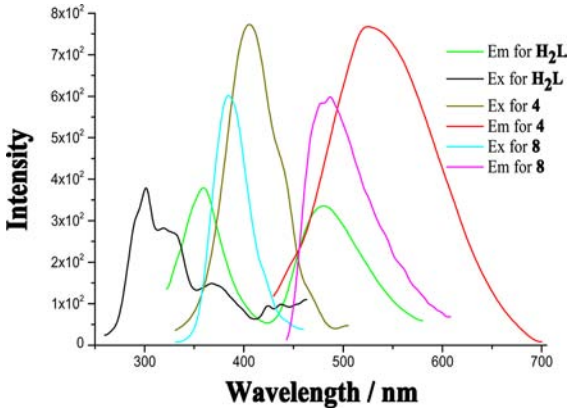

Figure 5. Visible emission and excitation spectra of the ligand $\mathbf{H_2L}$ and complexes **4** and **8** in MeCN solution at 1×10^{-5} M at room temperature.

state of the chromophores.[29] In dilute MeCN solution at 77 K, compared with that (λ_{em} = 526 nm, τ = 0.77 ns and ϕ = 0.67 × 10^{-3}) at room temperature on the same condition, complex **4** exhibits the strengthened fluorescence, which shows the higher luminescent intensity (λ_{em} = 507 and 565 nm) and the distinctively longer luminescence lifetimes (3.2 ns and 7.5 ms). This result demonstrates that the sensitization of the NIR luminescence for complexes **1**−**2** should arise from both the ^{1}LC (19 734 cm^{-1}) and the ^{3}LC (17 699 cm^{-1}) excited state of the Schiff-base ligand $\mathbf{H_2L}$ at low temperature.[21] If the antennae luminescence lifetime of complex **4** is to represent the excited-state lifetime in the absence of the energy transfer, the energy transfer rate (k_{ET}) in complexes **1**−**3** can thus be calculated from $k_{ET} = 1/\tau_q - 1/\tau_u$,[30] where τ_q is the residual lifetime of the luminescent emission undergoing quenching by the respective Ln^{3+} ion, and τ_u is the unquenched lifetime in the reference complex **4**, so the energy transfer rates for the Ln^{3+} ions in complexes **1**−**3** may all be estimated to be above 5×10^8 s^{-1}, which could well imply the reason for the effective energy transfer for complexes **1**−**3**. Furthermore, from the viewpoint of the energy level match, in spite of the effective energy transfer also taking place in complex **3**, the larger energy gap between the energy-donating ^{3}LC level (17 699 cm^{-1}) and the emitting level ($^4I_{13/2}$) of Er^{3+} ion than those of complexes **1**−**2** results in the great nonradiative energy loss during the energy transfer, which should be the reason to the weak and unobservable luminescence in the range of 800−1800 nm for complex **3**.[31]

Moreover, for complexes **1**−**2**, the respective NIR luminescent decay curves obtained from time-resolved luminescent experiments can be fitted monoexponentially with time constant of microseconds (1.57 μs for **1** at 1068 nm and 14.77 μs for **2** at 979 nm), and the intrinsic quantum yield Φ_{Ln} (0.62% for **1** or 0.79% for **2**) of the Ln^{3+} emission may be estimated by $\Phi_{Ln} = \tau_{obs}/\tau_0$, where τ_{obs} is the observed emission lifetime and τ_0 is the "natural lifetime", viz. 0.25 and 2.0 ms for the Nd^{3+} and Yb^{3+} ions, respectively.[32] As to the relatively higher quantum efficiency of **2** (0.79%) than that of **1** (0.62%), although there is a slightly larger energy gap ($^2F_{5/2}$, 10215 cm^{-1}, ΔE = 7484 cm^{-1}) of Yb^{3+} ion in complex **2** than that ($^4F_{3/2}$, 9363 cm^{-1}, ΔE = 7336 cm^{-1}) of the Nd^{3+} ion in complex **1**, the excited state of the Nd^{3+} ion in complex **1** is more sensitive to quenching by the O−H oscillators of the coordinated μ_3-OH^- groups and the distant C−H or N−H oscillators of the Salen-type Schiff-base ligand $\mathbf{H_2L}$ around the Nd^{3+} ions, besides the quantity of accepting levels of the Nd^{3+} ion while only one for the Yb^{3+} ion.

The change of use of $Ln(OAc)_3$ instead of $LnCl_3$ results in structure changes from $Ln_4(Salen)_4$ to $Ln_4(Salen)_2$, and the different photophysical properties of complexes **5**−**8** are presented in Table 2 and Figures 5−7. As shown in Figure 6,

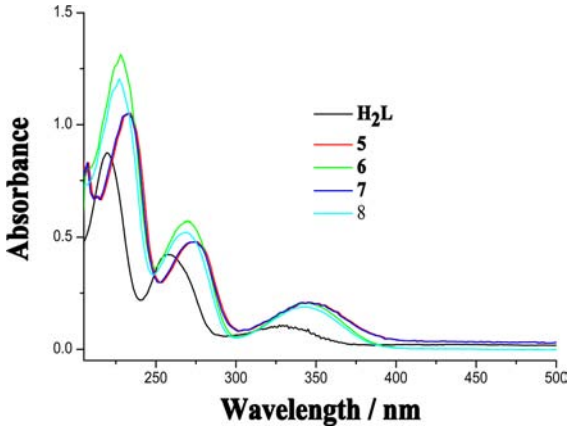

Figure 6. UV−vis absorption spectra of the ligand $\mathbf{H_2L}$ and complexes **5**−**8** in MeCN solution at 1×10^{-5} M at room temperature.

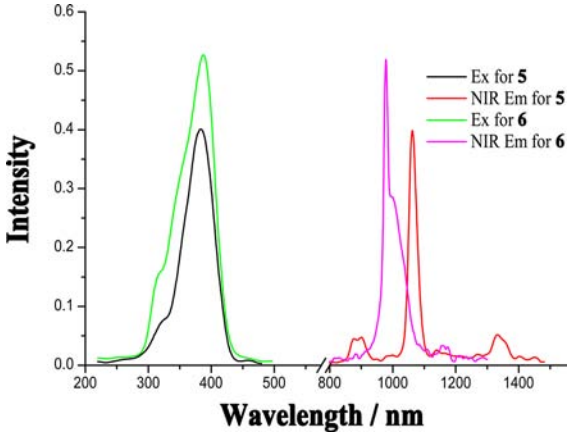

Figure 7. NIR emission and excitation spectra of complexes **5**−**6** in MeCN solution at 1×10^{-5} M at room temperature.

dx.doi.org/10.1021/ic300918c | Inorg. Chem. 2012, 51, 11377−11386

although the absorption spectra of complexes **5**−**8** are also red-shifted relative to that of the free ligand H_2L, the molar absorption coefficients of complexes **5**−**8** in all the lowest energy bands (343−346 nm) are almost 2 not 4 orders of magnitude larger than that (332 nm) of the ligand H_2L due to the involvement of two chromophores. For complexes **5**−**6**, the very weak residual visible emissions (λ_{em} = 483−490 nm, τ < 1 ns, and $\Phi_{em} < 10^{-5}$) and the characteristic NIR emission of the Nd^{3+} ion ($^4F_{3/2} \rightarrow {}^4I_{J/2}$, J = 9, 11, 13) or the Yb^{3+} ion ($^2F_{5/2} \rightarrow {}^2F_{7/2}$) also suggests that the sensitization from the chromophores to these Ln^{3+} ions takes place efficiently. Through the further investigation on the emission of the reference compound **8**, especially at 77 K, the strong fluorescence (λ_{em} = 473 nm, τ = 2.5 ns and 552 nm, τ = 6.5 ms) demonstrates that the sensitization of the NIR luminescence for complexes **5**−**6** should also arise from both the ^{1}LC (21 142 cm^{-1}) and the ^{3}LC (18 116 cm^{-1}) excited state of the Schiff-base ligand H_2L. Similar to that of complex **3**, no characteristic NIR emission of the Er^{3+} ion for complex **7** is observed due to the larger energy gap between the energy-donating ^{3}LC level (18 116 cm^{-1}) and the emitting level ($^4I_{13/2}$) of Er^{3+} ion. As to the relatively lower NIR intrinsic quantum yields of $Ln_4(Salen)_2$ complexes **5**−**6** (0.58% for **5** and 0.69% for **6**) than those of the corresponding $Ln_4(Salen)_4$ complexes **1**−**2** (0.62% for **1** and 0.79% for **2**), one of the reasons should be due to the larger energy gaps (ΔE = 8709 cm^{-1} for **5** and ΔE = 7891 cm^{-1} for **6**) in complexes **5**−**6** than those (ΔE = 7336 cm^{-1} for **1** and ΔE = 7484 cm^{-1} for **2**) of the Ln^{3+} ion in complexes **1**−**2**, and the other should arise from additional quenching effects by the nearby C−H oscillators of the monodentate and bidentate coordinated OAc^- groups around the Ln^{3+} ions. It is worth noting that the relatively larger NIR intrinsic quantum yields for both complexes **1**−**2** and complexes **5**−**6** than those of binuclear triple-decker or trinuclear triple-decker lanthanide (Nd^{3+} or Yb^{3+}) complexes[15] based on the typical Salen-type Schiff-base ligand with the rigid linker should result from the sensitization of the NIR luminescence from both the ^{1}LC and the ^{3}LC excited state of the flexible Schiff-base ligand H_2L for complexes **1**−**2** and **5**−**6**, and the decrease of the luminescent quenching effect by the coordinated MeOH solvates around the Ln^{3+} ions for the triple-decker Ln^{3+} complexes.

Magnetic Properties of Lanthanide Complexes. The direct-current (dc) magnetic measurements were performed on polycrystalline samples of $Ln_4(Salen)_4$ complexes **1**−**4** and $Ln_4(Salen)_2$ complexes **5**−**8** between 1.8 and 300 K under an external field of 1000 Oe, shown in Figures 8 and 9, respectively, where the observed paramagnetic behaviors of the two series of eight complexes arise from the Ln^{3+} (Ln = Nd, Yb, Er, or Gd) ions. For complexes **1**−**2** or **5**−**6**, the observed values of χ_mT at 300 K are 4.79 and 8.72 or 7.50 and 8.55 cm^3 K mol^{-1}, respectively, slightly smaller than the respective expected value for four noninteracting Nd^{3+} (6.56 cm^3 K mol^{-1}, $^4I_{9/2}$, S = 3/2, L = 6, g = 8/11) or Yb^{3+} (10.28 cm^3 K mol^{-1}, $^2F_{7/2}$, S = 1/2, L = 3, g = 8/7) ions.[33] On cooling, each χ_mT value gradually decreases, and the experimental values at 1.8 K of 1.72, 5.39, 2.94, and 5.23 cm^3 K mol^{-1} are obtained for **1**, **2**, **5**, and **6**, respectively, which is mostly attributed to the progressive thermal depopulation of the excited-state Stark sublevels due to the crystal-field effects of Nd^{3+} or Yb^{3+} ions.[34] The χ_m^{-1} versus T data for complexes **1**−**2** and **5**−**6** in the range 1.8−300 K obey the Curie−Weiss law, with Curie constant C = 4.89 cm^3 mol^{-1} K and Weiss constant θ = −8.59 K for **1**, C = 8.98 cm^3 mol^{-1} K and θ = −9.72 K for **2**, C = 7.71 cm^3 mol^{-1} K and θ = −18.17 K for **5**, and C = 8.62 cm^3 mol^{-1} K and θ = −10.23 K for **6**, respectively (Figures 5−6S).

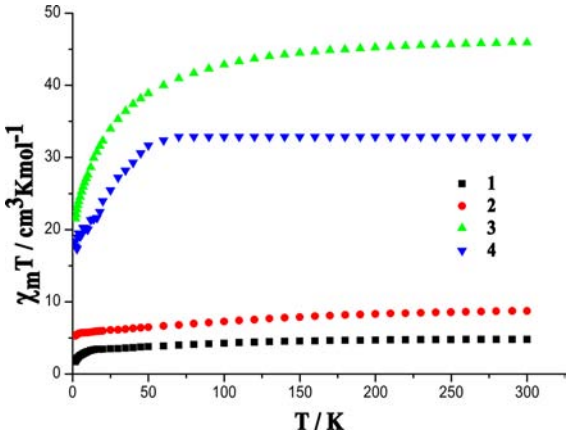

Figure 8. Temperature dependence of the χ_mT values for four $Ln_4(Salen)_4$ complexes **1**−**4** with an applied field of 1000 Oe.

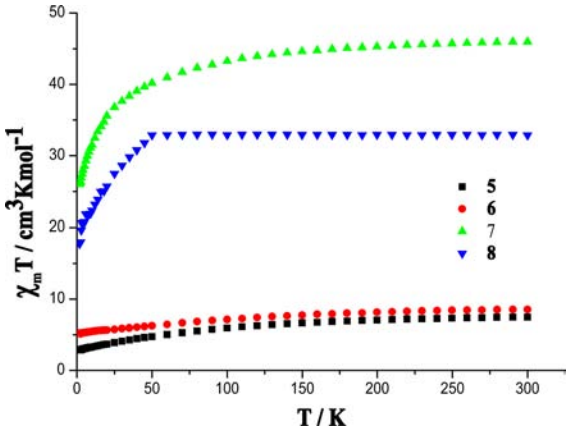

Figure 9. Temperature dependence of the χ_mT values for four $Ln_4(Salen)_2$ complexes **5**−**8** with an applied field of 1000 Oe.

As to complexes **3**−**4** and **7**−**8**, the observed χ_mT values of 45.92 and 45.97 cm^3 K mol^{-1} for the two Er^{3+} complexes **3** and **7**, 32.89 and 32.88 cm^3 K mol^{-1} for the two Gd^{3+} complexes **4** and **8**, respectively, are close to the theoretical value for four noninteracting Er^{3+} (45.92 cm^3 K mol^{-1}, $^4I_{15/2}$, S = 3/2, L = 6, g = 6/5) or Gd^{3+} (31.52 cm^3 K mol^{-1}, $^8S_{7/2}$, S = 7/2, L = 0, g = 2) ions.[33] Upon decreasing the temperature the χ_mT values remain fairly constant down to ∼60 K for **4** and **8** before dropping rapidly down to ca. 17.70 cm^3 K mol^{-1} at 1.8 K. The χ_m^{-1} versus T for complex **4** or **8** also obeys the Curie−Weiss law, with C = 33.57 cm^3 mol^{-1} K and θ = −4.47 K for **4** and C = 33.43 cm^3 mol^{-1} K and θ = −3.18 K for **8**, respectively (Figures 5−6S). Due to the isotropic nature of Gd^{3+} ions it is reasonable to assume the latter behavior is indicative of intramolecular antiferromagnetic interactions.[35] In the case of the Er^{3+} complexes **3** and **7**, although the χ_m^{-1} versus T also obeys the Curie−Weiss law, with C = 46.82 cm^3 mol^{-1} K and θ = −7.15 K for **3** and C = 46.51 cm^3 mol^{-1} K and θ = −5.29 K for **7**, respectively (Figures 5−6S), the negative deviation of χ_mT values starts to occur at slightly higher temperature (∼65 K) before reaching 21.52 and 26.22 cm^3 K mol^{-1}, respectively, at 1.8 K. This is most likely due to the combination of antiferromagnetic interactions, thermal depopulation of Stark sublevels, and the presence of significant magnetic anisotropy.[36]

dx.doi.org/10.1021/ic300918c | Inorg. Chem. 2012, 51, 11377−11386

CONCLUSIONS

Through the self-assembly of the flexible hexadentate Salen-type Schiff-base ligand $\mathbf{H_2L}$ with $LnCl_3{\cdot}6H_2O$ or $Ln(OAc)_3{\cdot}6H_2O$ (Ln = Nd, Yb, Er, or Gd), two series of homoleptic cyclic tetranuclear $[Ln_4(L)_2(HL)_2(\mu_3\text{-}OH)_2Cl_2]{\cdot}2Cl$ ($Ln_4(Salen)_4$, Ln = Nd, **1**; Ln = Yb, **2**; Ln = Er, **3**; Ln = Gd, **4**) and $[Ln_4(L)_2(\mu_3\text{-}OH)_2(OAc)_6]$ ($Ln_4(Salen)_2$, Ln = Nd, **5**; Ln = Yb, **6**; Ln = Er, **7**; Ln = Gd, **8**) are obtained, respectively. The self-assembly of polynuclear Ln^{3+} complexes provides an opportunity to tune the magnetic properties by anion-inducement. Moreover, the results of their photophysical studies show that more Salen-type Schiff-base ligands may work as antennae or chromophores for the sensitization of NIR luminescence of Nd^{3+} and Yb^{3+} ions, and the characteristic NIR luminescence with emissive lifetimes in the microsecond ranges has been sensitized from the excited state (both ^{1}LC and ^{3}LC) of the ligand due to the effective intramolecular energy transfer in complexes **1**−**2** and **6**−**7**. Moreover, the energy level's match between the excited states (^{3}LC) of the chromophores to the corresponding Ln^{3+} ion's exciting state is required for the enhancement of NIR luminescence, in addition to the avoiding or decreasing the luminescent quenching effect arising from OH-, CH-, or NH-oscillators around the Ln^{3+} ion. The specific design of polynuclear complexes from the flexible Salen-type Schiff-base ligands in facilitating the NIR sensitization and promoting intramolecular magnetic interactions is now under way.

ASSOCIATED CONTENT

Supporting Information

Crystallographic files of complexes **1**·6EtOH, **4**·2EtOH·$2H_2O$, and **6**−**7** in CIF format; selected bond lengths and angles for complexes **1**·6EtOH, **4**·2EtOH·$2H_2O$, and **6**−**7**; the intramolecular N−H···O H-bond interaction for complexes **1**·6EtOH; the perspective drawing of the cationic part in complex **4**·2EtOH·$2H_2O$; the intramolecular N−H···O H-bond interaction for **4**·2EtOH·$2H_2O$; and perspective drawing of complex **7**. Plots of χ_m^{-1} versus T for complexes **1**−**4** and **5**−**8** at 1000 Oe at the temperature range 1.8−300 K. This material is available free of charge via the Internet at http://pubs.acs.org.

AUTHOR INFORMATION

Corresponding Author

*E-mail: lvxq@nwu.edu.cn (X.L.), wkwong@hkbu.edu.hk (W.-K.W.). Phone: 86-29-88302312(o) (X.L.), 862-34117348(o) (W.-K.W.).

Notes

The authors declare no competing financial interest.

ACKNOWLEDGMENTS

This work is funded by the National Natural Science Foundation (21173165, 20871098), the Program for New Century Excellent Talents in University from the Ministry of Education of China (NCET-10-0936), the research fund for the Doctoral Program (20116101110003) of Higher Education of China, the State Key Laboratory of Structure Chemistry (20100014), the Education Committee Foundation of Shaanxi Province (11JK0588), Hong Kong Research Grants Council (HKBU 202407 and FRG/06-07/II-16) in P. R. China, the Robert A. Welch Foundation (Grant F-816), the Texas Higher Education Coordinating Board (ARP 003658-0010-2006), and the Petroleum Research Fund, administered by the American Chemical Society (47014-AC5).

REFERENCES

(1) (a) Artizzu, F.; Mercuri, M. L.; Serpe, A.; Deplano, P. *Coord. Chem. Rev.* **2011**, *255*, 2514−2529. (b) Armelao, L.; Quici, S.; Barigelletti, F.; Accorsi, G.; Bottaro, G.; Cavazzini, M.; Tondello, E. *Coord. Chem. Rev.* **2010**, *254*, 487−505. (c) Katkova, M. A.; Bochkarev, M. N. *Dalton Trans.* **2010**, 6599−6612. (d) Kido, J.; Okamoto, Y. *Chem. Rev.* **2002**, *102*, 2357−2368.

(2) Sessoli, R.; Powell, A. K. *Coord. Chem. Rev.* **2009**, *253*, 2328−2341.

(3) (a) Cable, M. L.; Levine, D. J.; Kirby, J. P.; Gray, H. B.; Ponce, A. *Adv. Inorg. Chem.* **2011**, *63*, 1−45. (b) Bünzli, J. C. G. *Chem. Rev.* **2010**, *110*, 2729−2755. (c) Bünzli, J. C. G.; Eliseeva, S. V. *J. Rare Earths* **2010**, *28*, 824−842. (d) Motson, G. R.; Fleming, J. S.; Brooker, S. *Adv. Inorg. Chem.* **2004**, *55*, 361−432.

(4) (a) Tanner, P. A.; Duan, C. K. *Coord. Chem. Rev.* **2010**, *254*, 3026−3029. (b) Moore, E. G.; Samuel, A. P. S.; Raymond, K. N. *Acc. Chem. Res.* **2009**, *42*, 542−552.

(5) (a) Rocha, J.; Carlos, L. D.; Paz, F. A. A.; Ananias, D. *Chem. Soc. Rev.* **2011**, *40*, 926−940. (b) Chen, F. F.; Chen, Z. Q.; Bian, Z. Q.; Huang, C. H. *Coord. Chem. Rev.* **2010**, *254*, 991−1010. (c) Swavey, S.; Swavey, R. *Coord. Chem. Rev.* **2009**, *253*, 2627−2638. (d) Ward., M. D. *Coord. Chem. Rev.* **2007**, *251*, 1663−1677.

(6) (a) Fan, W. Q.; Feng, J.; Song, S. Y.; Lei, Y. Q.; Zhou, L.; Zheng, G. L.; Dang, S.; Wang, S.; Zhang, H. J. *Nanoscale* **2010**, *2*, 2096−2103. (b) Tsukube, H.; Suzuki, Y.; Sykes, D.; Kataoka, Y.; Shinoda, S. *Chem. Commun.* **2007**, 2533−2535.

(7) Yang, X. P.; Jones, R. A.; Oye, M. M.; Wiester, M.; Lai, R. J. *New J. Chem.* **2011**, *35*, 310−318.

(8) Eliseeva, S. V.; Bünzli, J. C. G. *Chem. Soc. Rev.* **2010**, *39*, 189−227.

(9) (a) Bünzli, J. C. G.; Piguet, C. *Chem. Soc. Rev.* **2005**, *34*, 1048−1077. (b) Xu, H. B.; Chen, X. M.; Zhang, Q. S.; Zhang, L. Y.; Chen, Z. N. *Chem. Commun.* **2009**, 7318−7320. (c) Xu, H. B.; Li, J.; Zhang, L. Y.; Huang, X.; Li, B.; Chen, Z. N. *Cryst. Growth Des.* **2010**, *10*, 4101−4108.

(10) (a) Tang, J. K.; Hewitt, I.; Madhu, N. T.; Chastanet, G.; Wernsdorfer, W.; Anson, C. E.; Benelli, C.; Sessoli, R.; Powell, A. K. *Angew. Chem., Int. Ed.* **2006**, *45*, 1729−1733. (b) Lin., P. H.; Burchell, T. J.; Ungur, L.; Chibotaru, L. F.; Wernsdorfer, W.; Murugesu, M. *Angew. Chem., Int. Ed.* **2009**, *48*, 9489−9492. (c) Guo, Y. N.; Xu, G. F.; Guo, Y.; Tang, J. K. *Dalton Trans.* **2011**, *40*, 9953−9963.

(11) Lorenzo, S.; Cristiano, B.; Dante, G. *Chem. Soc. Rev.* **2011**, *40*, 3092−3104.

(12) (a) Wong, W. K.; Liang, H. Z.; Wong, W. Y.; Cai, Z. W.; Li, K. F.; Cheag, K. W. *New J. Chem.* **2002**, *26*, 275−278. (b) Lo, W. K.; Wong, W. K.; Wong, W. Y.; Guo, J. P.; Yeung, K. T.; Cheng, Y. K.; Yang, X. P.; Jones, R. A. *Inorg. Chem.* **2006**, *45*, 9315−9325. (c) Wong, W. K.; Yang, X. P.; Jones, R. A.; Rivers, J. H.; Lynch, V.; Lo, W. K.; Xiao, D.; Oye, M. M.; Holmes, A. L. *Inorg. Chem.* **2006**, *45*, 4340−4345. (d) Yang, X. P.; Jones, R. A.; Wong, W. K.; Oye, M. M.; Holmes, A. L. *Chem. Commun.* **2006**, 1836−1838. (e) Lü, X. Q.; Bi, W. Y.; Chai, W. L.; Song, J. R.; Meng, J. X.; Wong, W. Y.; Wong, W. K.; Jones, R. A. *New J. Chem.* **2008**, *32*, 127−131. (f) Zhao, S. S.; Lü, X. Q.; Hou, A. X.; Wong, W. Y.; Wong, W. K.; Yang, X. P.; Jones, R. A. *Dalton Trans.* **2009**, 9595−9602. (g) Bi, W. Y.; Wei, T.; Lü, X. Q.; Hui, Y. N.; Song, J. R.; Wong, W. K.; Jones, R. A. *New J. Chem.* **2009**, *33*, 2326−2334. (h) Lü, X. Q.; Feng, W. X.; Hui, Y. N.; Wei, T.; Song, J. R.; Zhao, S. S.; Wong, W. Y.; Wong, W. K.; Jones, R. A. *Eur. J. Inorg. Chem.* **2010**, 2714−2722. (i) Pasatoiu, T. D.; Madalan, A. M.; Kumke, M. U.; Tiseanu, C.; Andruh, M. *Inorg. Chem.* **2010**, *49*, 2310−2315.

(13) (a) Sakamoto, M.; Manseki, K.; Okawa, K. *Coord. Chem. Rev.* **2001**, *219*−*221*, 379−414. (b) Tanase, S.; Reedijk, J. *Coord. Chem. Rev.* **2006**, *250*, 2501−2510. (c) Andruh, M.; Costes, J. P.; Diaz, C.; Gao, S. *Inorg. Chem.* **2009**, *48*, 3342−3359.

(14) Costes, J. P.; Laussac, J. P.; Nicodème, F. *J. Chem. Soc., Dalton Trans.* **2002**, 2731−2736.

(15) Yan, P. F.; Chen, S.; Chen, P.; Zhang, J. W.; Li, G. M. *CrystEngComm* **2011**, *13*, 36−39.
(16) Yang, X. P.; Jones, R. A.; Wong, W. K. *Chem. Commun.* **2008**, 3266−3288.
(17) (a) Yang, X. P.; Jones, R. A.; Rivers, J. H.; Wong, W. K. *Dalton Trans.* **2009**, 10505−10510. (b) Wang, G. L.; Tian, Y. M.; Cao, D. X.; Yu, Y. S.; Sun, W. B. *Z. Anorg. Allg. Chem.* **2011**, *637*, 583−588.
(18) Yang, X. P.; Jones, R. A.; Oye, M. M.; Holmes, A. L.; Wong, W. K. *Cryst. Growth Des.* **2006**, *6*, 2122−2125.
(19) Yang, X. P.; Jones, R. A. *J. Am. Chem. Soc.* **2005**, *127*, 7686−7687.
(20) Yang, X. P.; Jones., R. A.; Wong, W. K. *Dalton Trans.* **2008**, 1676−1678.
(21) Feng, W. X.; Zhang, Y.; Lü, X. Q.; Hui, Y. N.; Shi, G. X.; Zou, D.; Song, J. R.; Fan, D. D.; Wong, W. K.; Jones, R. A. *CrystEngComm* **2012**, *14*, 3456−3463.
(22) (a) Long, J.; Habib, F.; Lin, P. H.; Korokov, I.; Enright, G.; Ungur, L.; Wernsdorfer, W.; Chibotaru, L. F.; Murugesu, M. *J. Am. Chem. Soc.* **2011**, *133*, 5319−5328. (b) Habib, F.; Lin, P. H.; Long, J.; Korobkov, I.; Wernsdorfer, W.; Murugesu, M. *J. Am. Chem. Soc.* **2011**, *133*, 8830−8833.
(23) Sheldrick, G. M. *SHELXL-97: Program for Crystal Structure Refinement*; University of Göttingen: Göttingen, Germany, 1997.
(24) Sheldrick, G. M. *SADABS*; University of Göttingen: Göttingen, Germany, 1996.
(25) Durig, J. R. *Vibrational Spectra and Structure: Application of FT-IR Spectroscopy*; Elsevier: Amsterdam, 1990.
(26) Mato-Iglesias, M.; Balogh, E.; Platas-Iglesias, C.; Toth, E.; de Blas, A.; Rodriguez, B. T. *Dalton Trans.* **2006**, 5404−5415.
(27) Nishioka, T.; Fukui, K.; Matsumoto, K. *Handbook on the Physics and Chemistry of Rare Earths*; Elsevier Science B. V.: Amsterdam, 2007.
(28) Comby, S.; Bünzli, J. C. G. *Handbook on the Physics and Chemistry of Rare Earths*; Elsevier Science B. V.: Amsterdam, 2007.
(29) Carnall, W. T.; Fields, P. R.; Rajnak, K. *J. Chem. Phys.* **1968**, *49*, 4443−4446.
(30) Dexter, D. L. *J. Chem. Phys.* **1953**, *21*, 836−850.
(31) Bünzli, J. C. G.; Comby, S.; Chauvin, A. S.; Vandevyver, C. D. B. *J. Rare Earths* **2007**, *25*, 257−274.
(32) Mercyri, M. L.; Deplano, P.; Pilia, L.; Serpe, A.; Artizzu, F. *Coord. Chem. Rev.* **2010**, *254*, 1419−1433.
(33) (a) Millar, J. S.; Drillon, M. *Magnetism: Molecule to Materials*; Wiley-VCH: Weinheim, 2005; Vol. *V*. (b) Kahn, O. *Molecular Magnetism*; VCH Publishers: New York, 1993.
(34) Liu, J. L.; Yuan, K.; Leng, J. D.; Ungur, L.; Wernsdorfer, W.; Guo, F. S.; Chibotaru, L. F.; Tong, M. L. *Inorg. Chem.* **2012**, *51*, 8538−8544.
(35) Yan, P. F.; Lin, P. H.; Habib, F.; Aharen, T.; Murugesu, M.; Deng, Z. P.; Li, G. M.; Sun, W. B. *Inorg. Chem.* **2011**, *50*, 7059−7065.
(36) Koo, B. H.; Lim, K. S.; Ryu, D. W.; Lee, W. R.; Koh, E. K.; Hong, C. S. *Chem. Commun.* **2012**, *48*, 2519−2521.